Characterization of Transient Induced Current Events in Ground Magnetometer Data

Brett A. McCuen[1], **Mark B. Moldwin**[1], **Mark Engebretson**[2]

[1]University of Michigan, Ann Arbor, Michigan
[2]Augsburg University, Minneapolis, Minnesota

Key Points:

- Short-timescale (< 60 s) geomagnetic perturbation events found at 6 high-latitude MACCS stations throughout 2015 are characterized.
- The existence of large-amplitude dB/dt at Earth's surface with timescale 1-10 seconds is demonstrated.
- Main space weather drivers and timescale of events suggest transient induced currents are different than typical GIC.

Corresponding author: =name=, `=email address=`

Abstract

We present a characterization of large amplitude, short-timescale geomagnetic disturbances that we refer to as transient induced current (TIC) events. TIC events are defined as one or more short-timescale ($<$ 60 seconds) dB/dt signature with magnitude $\geq$ 6 nT/s. We identified 40 TIC events that occurred at six stations of the Magnetometer Array for Cusp and Cleft Studies throughout 2015 and we demonstrate the existence of large-amplitude dB/dt with timescale less than 10 seconds in nine of the events. The association of these events to sudden commencements is weaker than expected, rather the events are more likely to occur in relation to substorm onsets. However, 15% of TIC events show no direct association to geomagnetic storms, substorms or nighttime magnetic impulse events. Our findings suggest that the TICs have different properties than typical geomagnetically induced currents and may be hazardous to conductive components of the Internet of Things network.

Plain Language Summary

Severe space weather events like geomagnetic storms and substorms cause large disturbances of the surface magnetic field that generate geomagnetically induced currents (GIC) in electrically conducting material on Earth. Large GICs capable of damaging transformers and causing large-scale power grid failure generally have timescales of minutes to tens of minutes and short-timescale ($<$ 1 minute) induced currents have not been considered a substantial threat. However, recent evidence suggests that transient induced currents (TIC) caused by second-timescale surface magnetic field perturbations are a potential hazard to technological infrastructure and may have an alternate coupling mechanism than typical GIC. In this study, we identify these TIC events in ground magnetometer data from the Magnetometer Array for Cusp and Cleft Studies (MACCS) throughout 2015. We characterize a set of these large-amplitude, short-timescale ($<$ 1 minute) surface magnetic field disturbances and investigate their association to space weather events in order to better understand their impact on electrical systems on Earth.

1 Introduction

Extreme geomagnetically induced currents (GIC) are a result of large-amplitude surface geomagnetic disturbances caused by space weather events. GICs can be large enough to cause damage to transformers resulting in major power outages and costly equipment damage (Pulkkinen et al., 2017). The time derivative of the surface magnetic field, dB/dt, is often used to study GICs in an effort to mitigate potential hazards and safeguard power systems. Based on the amplitude, timescale and observed dB/dt signatures, GICs can be characterized by their drivers in the magnetosphere-ionosphere (M-I) system. Transient GICs caused by second-timescale surface dB/dts are generally attributed only to sudden commencements (SC) as an M-I driver (Kataoka & Ngwira, 2016). However, several studies suggest that there are more complex, small-scale and localized processes involved in generating some extreme GICs (e.g., Engebretson et al., 2019; Ngwira et al., 2015, 2018). There is evidence to suggest that SCs are not the only driver for large-amplitude transient dB/dt at the surface; a study by Simpson (2011) concluded that rapid ionospheric current fluctuations of order 1-second can induce substantial currents in power transmission lines and may be capable of coupling directly to them, independent of ground conductivity. This behavior is different than typical GICs that enter power systems through the ground and are strongly dependent on ground conductivity. While these short-timescale magnetic field disturbances have been previously considered insubstantial in contributing to harmful GICs, this evidence suggests that they may cause transient induced currents (TIC) that are a potential hazard to technological infrastructure.

Simpson's conclusions prompted this investigation of TIC events to verify that they exist, characterize their behavior and assess the potential threat to technology and power systems on Earth. TICs are of the same frequency domain as electromagnetic pulses (EMP) of both natural (lightning) and anthropogenic (nuclear) causes. Power systems are generally equipped with surge protection and are less susceptible to heating caused by high-frequency, transient EMPs due to the minute-scale transformer thermal response time (Pulkkinen et al., 2017), but TICs could still pose a threat. A large TIC could first damage surge protection or monitoring circuits allowing longer-period induced currents to impact the system. Further, while many devices are equipped with surge protection, free-floating electronic devices without this feature are becoming more common as the Internet of Things (IoT) network rapidly grows. The IoT is an emerging network of objects equipped with sensors, actuators, and devices enabling communication with one another via the internet. IoT devices are connecting existing objects while also being implemented in applications to monitor and record environmental data in urban and rural environments. The absence of surge protection on low-cost devices like sensors makes them susceptible to damage by TICs (Johnson, 2016), and the lower operating voltages of these devices make them more sensitive to short-time voltage spikes as a result of TICs. The IoT network is growing at a rapid rate, with a projection of 18-billion connected devices related to IoT by 2022 (Moller, 2018). As the IoT network is continuously integrated into smart systems, the impacts of system failure become increasingly disruptive and even harmful to society. The need to evaluate potential risks to the IoT network is now more important than ever. In this study we surveyed short-timescale geomagnetic disturbances that may cause TICs and determined their frequency of occurrence, temporal dependence and relation (or lack thereof) to space weather events like geomagnetic storms and substorms.

2 Data Set and Identification Technique

The data used in this study are from six ground magnetometer stations of the Magnetometer Array for Cusp and Cleft Studies (MACCS). The stations are located in northeast Nunavut, Canada, shown on the map in Figure 1 in corrected geomagnetic (CGM) coordinates. The CGM coordinates were calculated for the year of 2015 with the IGRF transformation tool of the World Data Center (WDC) for Geomagnetism, Kyoto (geographic and CGM coordinates are listed in Supporting Information). The MACCS magnetometers collect 8 samples per second in three axes, then averages and records the data at two samples per second (Hughes and Engebretson, 1997). The half-second sampling rate and high sensitivity (0.01 nT resolution) of the MACCS magnetometers is sufficient to detect shorter period Pc 1 and 2 pulsations. The magnetometers are aligned with the magnetic field so that the x-component is in the north-south direction.

A semi-automated algorithm was developed to identify dB/dt signatures in the magnetometer data with user-specified duration and magnitude. The algorithm searches for changes in the slope of the magnetic field in each axis separately and ignores fluctuations lasting less than 1 second. We used this to identify dB/dt signatures with magnitude 6 nT/s or higher and duration less than 1 minute. The dB/dt threshold is comparable to the surface magnetic field perturbations (approximately ± 8 nT/s) that caused the HydroQuebec power grid to fail during the geomagnetic storm of March 1989 (Kappenman, 2006). TIC events are then characterized as an occurrence of one or more of these dB/dts, grouped together if they occur within 1 hour of another (regardless of the axis measured in and the station measured at). Because of the timescale and magnitude of the dB/dts sought, many of these signatures are similar in nature to magnetometer noise caused either by instrumental artifacts or magnetic deviation due to by interference by ferromagnetic materials in the vicinity of the magnetometer (Nguyen et al., 2020). Thus, each event returned from the routine was visually inspected to confirm that it appeared to be of physical nature or remove it if it was a result of noise. After the filtering process,

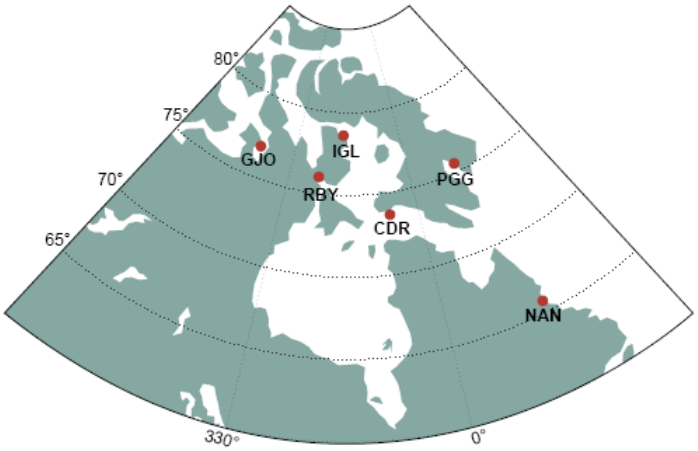

Figure 1: Map of the six MACCS stations used in this study with grid lines in corrected geomagnetic coordinates. Station locations are given in Table 1.

a total of 181 *dB/dt* signatures were identified. The majority (∼63%) of these signatures were measured in the x-component, 29.5% in the y-component and 7.5% in the z-component. Finally, grouping the *dB/dt*s if they occurred within 1 hour of another signature resulted in 40 TIC events.

While the primary temporal periods of interest in this study are 1-60 seconds, we also ran the algorithm with the upper limit for the duration of events extended to 5 minutes in order to compare to the 5-10 minute lasting magnetic impulse events (MIE) studied in Engebretson et al. (2019). Note that we used raw magnetic field data in this study and typical GIC identification involves smoothing the magnetometer data prior to searching for large *dB/dt*s. Because our identification method relies on changes of the magnetic field lasting at least 1 second, some larger and more extended *dB/dt*s are undetected by our algorithm due to more rapid changes within. We also found that the events resulting from magnetometer noise have several characteristics that make them possible to automatically detect; our future work will incorporate a comprehensive noise identification method in the algorithm.

3 Occurrence of TIC Events

We identified 40 TIC events consisting of one or more *dB/dt* signatures with magnitude 6 nT/s or higher and duration less than 60 seconds. We expected to find many TIC events occurring due to SCs as they have been considered the primary driver for the most rapid and extreme induced currents (Kataoka & Ngwira, 2016). However, we found only one SC-related event despite five recorded SCs in 2015 that occurred when the MACCS stations were located on the dayside (the other four SCs caused *dB/dt*s at the MACCS stations that all lasted less than 60 seconds but did not exceed the 6 nT/s threshold. Source: Kakioka Magnetic Observatory. www.kakioka-jma.go.jp). This SC-related event, shown in Figure 2a, started on 22 June 2015 at 18:33:22 UT (12:41:22 MLT, at RBY), just seconds after a large CME reached Earth causing an SSC at 18:33 UT. The largest *dB/dt* signature of the entire data set occurred in this event at RBY in the y-component, lasting 9.5 seconds with a magnitude of -33.49 nT/s. The *dB/dt*s measured in the y- and z-components at PGG and CDR all last 10.5 seconds or less, with the shortest event in the y-component at CDR with a magnitude of 13.3 nT/s and lasting just 5 seconds. All four stations were on the dayside during the time of the event. The hol-

low circles in all three panels of Figure 2 mark the start of each dB/dt within the TIC event and the solid dots mark the end. Note that axes in all plots of Figure 2 have been adjusted by subtracting the mean $B_{x,y,z}$ value from the interval, so the magnitude of the rate of change of the magnetic field is still to scale.

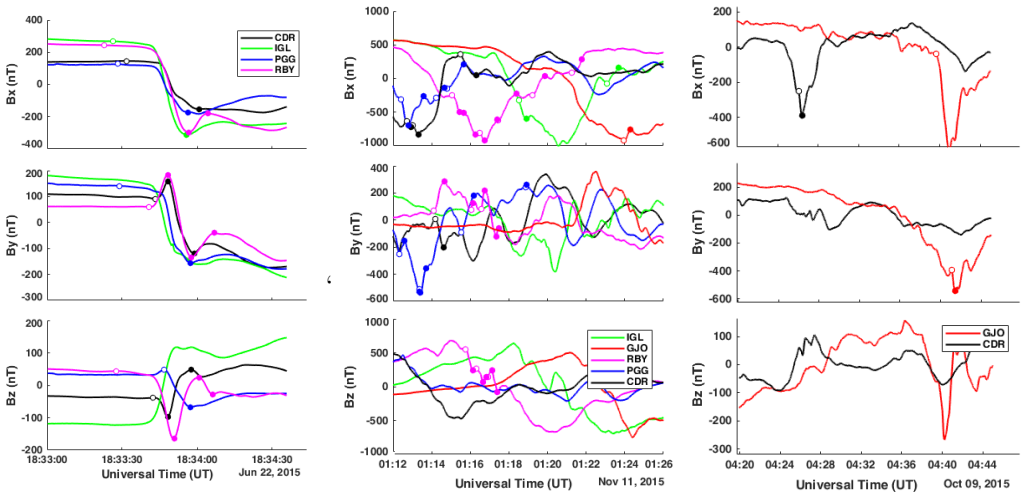

(a) (b) (c)

Figure 2: (a): A TIC event that occurred on 22 June 2015. (b): An event that occurred on 11 November 2015. (c) An event that occurred on 9 October 2015. All three panels show the x, y and z components of the surface magnetic field from top to bottom, respectively. Hollow circles mark the start of a dB/dt signature and the dots mark the end.

Shown in Figure 2b is a TIC event that occurred on 11 November 2015 beginning at 01:12:20 UT (21:22:36 MLT of 10 November 2015). This event consists of 34 dB/dts measured at all but the NAN station. Of these 34 dB/dts, six have magnitude greater than 10 nT/s and five have duration $<$ 10 seconds. One of the largest dB/dts (16.2 nT/s) was measured at PGG at 1:13:21 UT in the y-component and lasted only 1 second. The overall event lasts about 10 minutes and occurs within a larger, longer ($\sim$1 hour) magnetic impulse event (MIE) that is investigated by Engebretson et al. (2019). The MIE and the TIC event are not associated with a geomagnetic storm, although a substorm onset occurred at 01:07 UT, about 5 minutes prior to the start of the event. The MIE was preceded by a steady magnetic field for at least an hour prior to the start of the disturbance around 00:40 UT.

Finally, Figure 2c shows a TIC event on 9 October 2015 starting at 04:26:06 UT at the CDR station (23:31:06 MLT of 8 October 2015) where B_x decreases by 135.9 nT in 21 seconds (dB_x/dt = -6.46 nT/s). Then about 14 minutes later, two similar signatures occurred at GJO: a dB_x/dt of -6.87 nT/s at 04:49:37 UT and a dB_y/dt of -6.52 nT/s at 04:41:05 UT. Note, however, that the dB_x/dt at GJO actually lasted 80 seconds, this is one of the signatures identified when extending the upper threshold for the duration of the signatures in the search algorithm to 5 minutes rather than 60 seconds. This TIC event occurred on the second day of recovery from a moderate geomagnetic storm (the SuperMAG Ring Current (SMR) index reached -123 nT in hour 23 of 7 October but recovered to around -34 nT during the hour of the event on 9 October) and there were marked substorm onsets occurring at 04:13 UT and 4:34 UT. Further, a nighttime MIE was identified at RBY at 04:37 UT but was not identified at CDR (note that GJO, the other sta-

tion that measured this TIC event was not one of the stations used in the statistical study of Engebretson et al., 2019). There did occur a nighttime MIE measured at CDR later on at 22:00 UT of 9 October, and while no TIC signatures were identified at CDR during this time, a TIC event (dB_x/dt = -10.43 nT/s) was identified at PGG at 21:56:02 UT, preceding that MIE by several seconds.

We demonstrate the existence of significant magnetic disturbances with timescale $\leq$ 10 seconds in nine of the 40 TIC events identified. In five of these events, the shortest-timescale signatures exhibit the largest amplitude disturbances of the entire set of events ($|dB/dt| \geq$ 10 nT/s). Further, there are seven cases in which these signatures precede a larger, longer timescale (< 60 seconds) *dB/dt*. Examples of these signatures can be seen in Figure 2a (B_y at RBY: dB_y/dt = -33.49 nT/s), and in Figure 2b (the decrease in *By* at CDR at 18:33:43 UT lasts for 5 seconds and has rate of change of 13.23 nT/s; the two signatures in the z-component at CDR last 6 and 9.5 seconds with magnitudes of -9.85 and 15.28 nT/s, respectively).

4 Spatial and Temporal Characteristics and Space Weather Dependence

Of the 40 identified events, 27.5% consist of at least one *dB/dt* signature with magnitude exceeding 10 nT/s and half of these occurred within an event that has at least one other $|dB/dt| \geq$ 10 nT/s. These ten largest events were measured primarily between 64° and 66° geographic latitude at the PGG and CDR stations: PGG and CDR not only recorded the majority of the largest events but a substantial fraction (50% and 43%, respectively) of events in general. The GJO (76.86°) station recorded 9 events and RBY (75.62°) and IGL (78.63°) recorded 3 and 4 events, respectively. The southern-most station, NAN (65.67°), recorded just two events that were not recorded at any other station. In fact, 75% of the events were measured locally at only one station (the average, absolute distance from one station to the nearest station is ∼580 km. Note this average excludes NAN as it is the lowest latitude station with only two locally recorded events). Of the other 25% of events measured at more than one station, 4 were recorded relatively simultaneously (as shown in Figures 2a and 2b) while 6 other events had *dB/dt*s at more than one station delayed by at least 2 minutes (and at most 14 minutes, shown in Figure 2c).

TIC events occurred substantially more often in the Fall-Winter months with exactly 60% of events occurring in October through December. To illustrate the occurrence of TIC events as a function of magnetic local time as well as the association to geomagnetic storms and substorms, Figure 3 shows the maximum *dB/dt* of each TIC event throughout 2015 as a function of MLT. The events that occurred between 18-6 MLT are plotted as squares with opacity according to temporal proximity of prior substorm onset: the black squares signify that the event started within 15 minutes after the nearest substorm onset and during nighttime hours of 18-6 MLT, the grey squares are events that occurred 15-30 minutes after substorm onset and the white squares occurred more than 30 minutes after the nearest substorm onset (daytime events were automatically marked as white squares). These onset delays were determined with the SuperMAG substorm event list. The bars extending from some of the squares in Figure 3 signify the full duration of the event if it consisted of multiple *dB/dt*s, showing at what point throughout the event that the maximum *dB/dt* occurred. Only three events occurred in the commencement or main phase of a geomagnetic storm, these are labeled in Figure 3. There are also five events that occurred on the first day of recovery from a geomagnetic storm and four events that occurred on the second day of recovery.

Figure 3 shows that a vast majority (90%) of events occur at nighttime between 18-6 MLT with peak number of events (70%) in the pre-midnight sector from 18-24 MLT. A large number of the events (65%) occurred within 30 minutes of substorm onset, but

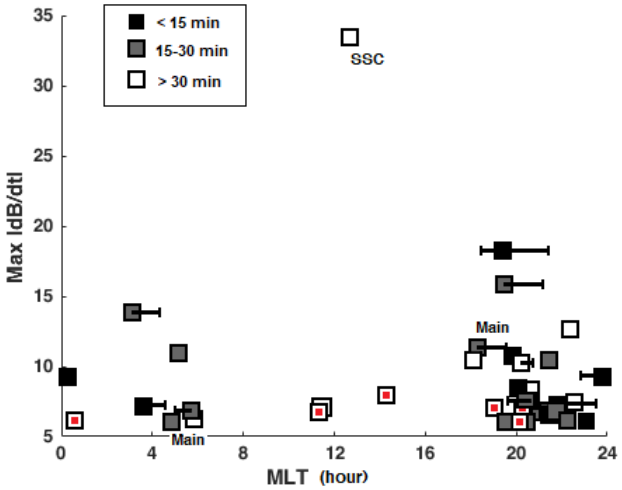

Figure 3: Maximum *dB/dt* as a function of magnetic local time (MLT) of each TIC event found in 2015. The bars extended from some squares signifies the duration of an event with multiple *dB/dt*s. The opacity of squares is based on the temporal proximity after the nearest substorm onset.

it is clear from Figure 3 that not all of the nighttime events show this association to substorm onsets (see white squares occurring at nighttime). While there is a strong association of TIC events to substorm onsets, 30% of events occurred more than 30 minutes after a substorm onset, with a small subset of events (6) that occurred more than 2 hours after substorm onset. Figure 3 also shows that the eleven *largest* TIC events ($\geq$ 10 nT/s) are more likely to occur between 18-24 MLT, but these are not necessarily more likely to occur within 30 minutes of substorm onset as about half of the set of largest events occurred more than 30 minutes after. As previously stated, five of these eleven largest events also have signatures lasting 10 seconds or less, with magnitude exceeding 10 nT/s. Comparison to the nighttime MIE events of Engebretson et al., (2019) found that 70% are related: either preceding the MIE within 30 minutes or occurring within the longer-timescale perturbation. Eight of the largest amplitude events were associated to a nighttime MIE. While the set of events exhibit a clear association to substorm activity and nighttime MIEs, there exists a subset of TIC events (15%) that occur more than 30 minutes prior to a nighttime MIE, more than 30 minutes after a substorm onset, and during relatively quiet geomagnetic conditions (i.e. not during any phase of a geomagnetic storm, nor ocurring within two days of recovery), we classify these as unrelated events. These six events are expressed in Figure 3 as squares with red dots in the center. None of these unrelated events are in the set of largest disturbances, but they do show more of a temporal spread than the majority of events as two of these unrelated events are within the only four events that occurred during the daytime.

5 Discussion and Conclusions

In this study, we surveyed short-timescale ($\leq$ 60 seconds) ground magnetic disturbances with magnitude of 6 nT/s or greater that occurred at six MACCS stations throughout 2015. We identified 40 events that consist of one or more of these *dB/dt*s. About a third of the events exceed 10 nT/s which is in the range of magnetic disturbances that can induce potentially damaging currents to technological infrastructure. While we identified a fairly small number of TIC events, the set exhibits several cases of large-amplitude ($\geq$ 10 nT/s) and very short-timescale ($\leq$ 10 s) disturbances. We found that SCs were

not the main driver for these transient magnetic disturbances, although the large SSC that occurred on 22 June did cause the largest amplitude perturbation, it was the only TIC event associated to an SC despite many occurring over the course of the year. Rather, TIC events occurred most often during local magnetic nighttime, with the highest frequency of events in the pre-midnight sector from 18-24 MLT. There is a clear association of these events to the onset of substorms as well as association to nighttime MIEs (about two-thirds occurring at nighttime within 30 minutes of substorm onset and about two-thirds related to MIEs), but there is not a perfect correlation between nighttime events and substorm-related events (i.e. not all nighttime events are substorm-related). Further, the relationship with substorm onsets appears to be a complicated one, as several events occurred multiple hours after the nearest substorm onset; this association will be investigated further in a future study extending the search for TIC events to many other stations and for a longer period of time.

In addition to a clear association to substorm onsets, we found that a majority of our events either preceded or occurred within a nighttime MIE (Engebretson et al., 2019). These nighttime MIEs are large-amplitude magnetic disturbances with 5-10 minute timescale occurring in this region of north-east Canada from 2014-2017. Like MIEs, the TIC events identified were often but not always associated with substorms on a similar two-thirds basis. Using the spherical elementary current systems (SECS) method (Amm & Viljanen, 1999) and the implementation of this technique by Weygand et al. (2011), a superposed epoch analysis was conducted to investigate the average equivalent ionospheric currents (EIC) and inferred field-aligned currents (FAC) during 21 nighttime MIEs that occurred at CDR from mid-2014 to 2016. Enebretson et al. (2019a) found that the largest of these MIEs were associated to intense westward ionospheric currents 100 km above CDR, coinciding with a region of shear between upward and downward FAC. They also found that the largest horizontal dB/dts occurred slightly south of CDR in a localized region of $\sim$275 km. Our TIC events show some similarities to these MIEs: 1) Of all six stations, the PGG and CDR stations measured the greatest number of events as well as the largest-amplitude TIC events ($|dB/dt| \geq$10 nT/s) and 2) we found only nine events that were measured by more than one station, so the majority of our events ($\sim$75%) were measured locally at just one station. The average distance from one of the six stations to the next nearest is about 580 km and the MACCS magnetometers generally have an approximate 300 km range of the sky above. Our future work will expand the data set to include more stations over an extended period of time and will include a superposed epoch analysis to investigate the ionospheric activity during TIC events.

In order to better understand our events in the context of these MIEs, we extended the upper threshold of the search algorithm to identify disturbances lasting up to 5 minutes with magnitude of 6 nT/s or greater. We found 25 additional dB/dts that were all related to TIC events that we had already identified and only one signature lasted slightly longer than 2 minutes. We hypothesized that the absence of magnetic perturbations in the 2-5 minute timescale range could be due to algorithm bias: because the method of the routine searches for changes in the direction of the slope (dB/dt) with the condition that the change last for at least 1 second and we used raw magnetic field data without any smoothing method, the algorithm could be missing collections of dB/dt signatures lasting 2-5 minutes because there are shorter timescale variations occurring within them that did not meet the threshold of 6 nT/s. To test this theory, we applied a 10-point moving mean on the magnetic field data so that any of these shorter variations would be smoothed over, then ran the search algorithm for disturbances lasting up to 5 minutes again. Engebretson et al. (2019) also used a 10-point moving average smoothing on the data. We found when the data were smoothed around 10-points, the algorithm identified all the same events as the raw data and identified 17 new events. All the events with signatures lasting $>$ 60 seconds were the same apart from one case where the smoothed data marked the magnetic field response to the SSC at RBY as a disturbance lasting 60.5 seconds rather than 34 seconds. This occurred in many cases where the smoothed data identified the

same signatures as longer events; because the algorithm searches for changes in the direction of the *dB/dt*, the 10-point smoothing was altering the exact moment that the slope changed sign and the signature started or ended. While the smoothing method resulted in many signatures marked as having longer duration, there was still only a small number of *dB/dt*s with > 1 minute timescale (32 as opposed to 25 with raw data) and the longest signature lasted 147 seconds. By comparing our results with smoothed data, we verified the methodology of the algorithm and determined that the absence of large-amplitude (≥ 6 nT/s) magnetic disturbances with timescale $\sim$2.5-5 minutes is not due to algorithm bias. This finding suggests that all longer-timescale magnetic perturbations at these stations consist of more rapid variations lasting less than 2.5 minutes, with a vast majority < 60 seconds.

While TIC events show a clear association with substorm activity as well as many shared characteristics with nighttime MIEs, the TICs are not consistently related to these space weather events. We found a small subset of TIC events that are unrelated to space weather events. The results of Ngwira et al. (2015) show that geoelectric fields during severe geomagnetic storms exhibit extreme local enhancements with spatial scale $\sim$250-1600 km. TIC events show a similar localized behavior with a weak association to geomagnetic storms, suggesting that there are other physical mechanisms, even beyond substorms, for localized peak enhancements in the geoelectric field (roughly proportional to the *dB/dt*). Finally, what we learned from the error analysis of this study is that a common smoothing method on the data altered the timing and amplitude of the events, suggesting that the short-timescale nature of the geomagnetic field could often be removed with common data processing methods, and we show that these signatures can have amplitude of the same order as longer-timescale events that are relevant to GICs. We will use our error analysis to characterize the noise and artifacts in the MACCS stations and other ground magnetometer arrays in order to fully automate the algorithm we developed and improve the accuracy of data cleaning techniques. The continued investigation of TICs is necessary to fully understand their behavior and the potential impacts they pose to technological infrastructure on Earth.

In summary, we identified many large-amplitude transient *dB/dt* signatures on the order of seconds that have the potential to induce substantial currents in conductors on the surface. We found many cases where these signatures preceded a nighttime MIE or occurred within the longer-timescale perturbation, which could pose a threat by damaging the surge protection on an electronic system and consequently allowing larger currents to flow through. Some TIC events, like that in Figure 2c, exhibit *dB/dt* signatures rapidly at one station and then even larger at another, which could demonstrate a horizontal ionospheric discharge similar to the modeled currents of Simpson (2011). The exact coupling mechanisms of these rapid currents to technological infrastructure are not well understood, but are suggested to couple directly to conductors on Earth instead of entering systems through the ground. In addition to expanding the data set to find more TIC events, a future experimental study will be conducted to investigate the coupling mechanisms of rapid ionospheric currents to conductors on the surface.

Acknowledgments

The authors thank the MACCS team for data. MACCS is operated by the University of Michigan and Augsburg University and funded by the U.S. National Science Foundation via grants AGS-2013433 and AGS-2013648.

We gratefully acknowledge the SuperMAG collaborators (http://supermag.jhuapl.edu/info/?page=acknowledgement)

The table of TIC events used in this study is available on the University of Michigan Deep Blue data repository (doi: pending review, table uploaded as .xlsx file as supplemental material for review).

References

Amm, O., & Viljanen, A. (1999). Ionospheric disturbance magnetic field continuation from the ground to the ionosphere using spherical elementary current systems. *Earth, Planets and Space*, *51*(6), 431–440. doi: 10.1186/BF03352247

Boteler, D. H., Pirjola, R. J., & Nevanlinna, H. (1998). The effects of geomagnetic disturbances on electrical systems at the Earth's surface. *Advances in Space Research*, *22*(1), 17–27. doi: 10.1016/S0273-1177(97)01096-X

Engebretson, M. J., Hughes, W. J., Alford, J. L., Zesta, E., Cahill, L. J., Arnoldy, R. L., & Reeves, G. D. (1995). Magnetometer array for cusp and cleft studies observations of the spatial extent of broadband ULF magnetic pulsations at cusp/cleft latitudes. *Journal of Geophysical Research*, *100*(A10), 19371. doi: 10.1029/95ja00768

Engebretson, M. J., Pilipenko, V. A., Ahmed, L. Y., Posch, J. L., Steinmetz, E. S., Moldwin, M. B., ... Vorobev, A. V. (2019). Nighttime Magnetic Perturbation Events Observed in Arctic Canada: 1. Survey and Statistical Analysis. *Journal of Geophysical Research: Space Physics*, *124*(9), 7442–7458. doi: 10.1029/2019JA026794

Engebretson, M. J., Steinmetz, E. S., Posch, J. L., Pilipenko, V. A., Moldwin, M. B., Connors, M. G., ... Kistler, L. M. (2019). Nighttime Magnetic Perturbation Events Observed in Arctic Canada: 2. Multiple-Instrument Observations. *Journal of Geophysical Research: Space Physics*, *124*(9), 7459–7476. doi: 10.1029/2019JA026797

Ganushkina, N. Y., Liemohn, M. W., & Dubyagin, S. (2018). Current Systems in the Earth's Magnetosphere. *Reviews of Geophysics*, *56*(2), 309–332. doi: 10.1002/2017RG000590

Gjerloev, J. W. (2012). The SuperMAG data processing technique. *Journal of Geophysical Research: Space Physics*, *117*(9), 1–19. doi: 10.1029/2012JA017683

Hughes, W., & Engebretson, M. (1997). MACCS: Magnetometer array for cusp and cleft studies. (1).

Johnson, D. (2016, Sep). *Circuit protection is essential to ensuring iot growth.* Bourns Inc. Retrieved from `http://www.electronicproducts.com/Passive_Components/Circuit_Protection/Circuit_protection_is_essential_to_ensuring_IoT_growth.aspx`

Kappenman, J. G. (2006). Great geomagnetic storms and extreme impulsive geomagnetic field disturbance events - An analysis of observational evidence including the great storm of May 1921. *Advances in Space Research*, *38*(2), 188–199. doi: 10.1016/j.asr.2005.08.055

Kataoka, R., & Ngwira, C. (2016). Extreme geomagnetically induced currents. , *3*(1). Retrieved from `http://dx.doi.org/10.1186/s40645-016-0101-x` doi: 10.1186/s40645-016-0101-x

Khomutov, S. Y., Mandrikova, O. V., Budilova, E. A., Arora, K., & Manjula, L. (2017). Noise in raw data from magnetic observatories. *Geoscientific Instrumentation, Methods and Data Systems*, *6*(2), 329–343. doi: 10.5194/gi-6-329-2017

Moller, R. (2018, June). *Ericsson mobility report* (Tech. Rep.). Ericsson Inc.

Newell, P. T., & Gjerloev, J. W. (2011). Substorm and magnetosphere characteristic scales inferred from the SuperMAG auroral electrojet indices. *Journal of Geophysical Research: Space Physics*, *116*(12), 1–15. doi: 10.1029/2011JA016936

Newell, P. T., & Gjerloev, J. W. (2012). SuperMAG-based partial ring current indices. *Journal of Geophysical Research: Space Physics*, *117*(5), 1–15. doi: 10

.1029/2012JA017586

Nguyen, N., Muller, P., & Collin, J. (2020). The Statistical Analysis of Noise in Triaxial Magnetometers and Calibration Procedure. *2019 16th Workshop on Positioning, Navigation and Communications (WPNC)*, 1–6. doi: 10.1109/wpnc47567.2019.8970255

Pulkkinen, A., Bernabeu, E., Thomson, A., Viljanen, A., Pirjola, R., Boteler, D., ... MacAlester, M. (2017). Geomagnetically induced currents: Science, engineering, and applications readiness. *Space Weather*, *15*(7), 828–856. doi: 10.1002/2016SW001501

Simpson, J. J. (2011). On the possibility of high-level transient coronal mass ejection-induced ionospheric current coupling to electric power grids. *Journal of Geophysical Research: Space Physics*, *116*(11), 1–12. doi: 10.1029/2011JA016830

Weygand, J. M., Amm, O., Viljanen, A., Angelopoulos, V., Murr, D., Engebretson, M. J., ... Mann, I. (2011). Application and validation of the spherical elementary currents systems technique for deriving ionospheric equivalent currents with the North American and Greenland ground magnetometer arrays. *Journal of Geophysical Research: Space Physics*, *116*(3), 1–8. doi: 10.1029/2010JA016177